Abstract Title Page
Not included in page count.

Title:

Graphical Models for Quasi-Experimental Designs

Authors and Affiliations:

Yongnam Kim, University of Wisconsin-Madison
Peter M. Steiner, University of Wisconsin-Madison
Courtney E. Hall, New Mexico Public Education Department
Dan Su, University of Wisconsin-Madison

Abstract Body

Limit 4 pages single-spaced.

Background / Context:

Experimental and quasi-experimental designs play a central role in estimating cause-effect relationships in education, psychology, and many other fields of the social and behavioral sciences. In implementing the designs for causal inference, researchers frequently rely on Campbell's tradition of ruling out threats to internal validity like selection, maturation, history, or instrumentation effects (Shadish, Cook & Campbell, 2002). Though the conceptualization of internal validity and its threats is useful from a practical point of view, a more formal representation of the designs helps in precisely defining the causal estimands of interest and in discussing the assumptions required for identifying the causal estimands. The Rubin Causal Model (RCM) with its potential outcomes frameworks (Holland, 1986) offers a very convenient way of defining causal estimands and deriving identification assumptions like the stable-unit-treatment-value assumption (SUTVA; Rubin, 1990), strong ignorability for propensity score matching designs (Rosenbaum & Rubin, 1983), or the monotonicity assumption for instrumental variable designs (Angrist, Imbens, & Rubin, 1996).

However, RCM is not the only way to formalize causal inference. Recently, graph-theoretical models that exploit substantive knowledge about the data-generating mechanism have become more popular for causal investigations in artificial intelligence, epidemiology or sociology (Morgan & Winship, 2012; Pearl, 2009; Spirtes, Glymour & Scheines, 2000). The graphical approach to causal inference is rather new to the social sciences like education and psychology, but an increasing number of researchers find graphical models appealing because they naturally convey substantive theories to causal graphs without relying on pure logical and mathematical expressions. Moreover, causal graphs also allow researchers to represent features of the study designs and data collection process that affect the identification of causal effects. This paper discusses the causal graphs for experimental and quasi-experimental designs and thereby provides a new perspective on the designs' mechanics and assumptions.

Purpose / Objective / Research Question / Focus of Study:

We investigate graphical models for experimental and quasi-experimental designs (Steiner et al, in press) and focus on the *nonparametric identification* of the causal effects (that is, without making any functional form or distributional assumptions). In particular, we present and discuss the causal graphs for randomized controlled trials (RCTs), regression discontinuity (RD) designs, instrumental variable (IV) designs, and matching and propensity score (PS) designs. For each design we show how the assumptions required for identifying a causal effect are encoded in the graphical representation. We believe that causal graphs make the assumptions more transparent and easier to understand for applied researchers. The causal graphs also reveal new insights about the quasi-experimental designs. For instance, the propensity score is a collider variable that offsets confounding bias via collider bias. Or, the conditional causal graphs for compliers, always takers and never takers of the IV design make it very clear why the causal effect is only identified for compliers.

Significance / Novelty of study:

In drawing causal graphs for different (quasi-)experimental designs, we introduce novel concepts and explanations of the designs' causal identifying mechanisms. For the RD design, we introduce the concept of a limiting graph at the cutoff score which directly explains why the average treatment effect at the cutoff score is nonparametrically identified while the treatment effects to the left and right of the cutoff score are not identifiable (without further assumptions). For the IV design, we provide a simple but formally precise graphical explanation of why the average treatment effect is identified only for compliers but not for always takers and never takers. From the IV graphs one can also directly see how the complier average treatment effect is computed from observed data consisted of the mixture population of those latent subgroups. Finally, for PS designs we demonstrate that the PS is a collider variable that offsets the confounding bias via collider bias. In addition to these novel formulations of quasi-experimental designs, a comparison of the designs' causal graphs impressively reveals that stronger designs (like RCTs or RD designs) results in simpler graphs due to researchers' increasing control over the assignment mechanism.

Usefulness / Applicability of Method:

The graphical representation of (quasi-)experiments helps practitioners in getting a better understanding of the designs' assumptions and limitations and, finally, in doing better causal studies. We also think that the causal graphs we present are a valuable tool for teaching (quasi)-experimental designs.

Findings / Results:

Figure 1(1) shows a typical data generating process for an observational study, where the *X*s represent the confounders that prevent a direct identification of the treatment's (*Z*) causal effect on the outcome (*Y*). Figure 1(2) shows a stylized graph of Figure 1(1), where **X** represents the set of confounders X_1 to X_3 while the other independent variables became a part of the independent error terms which are no longer shown. If not all confounders **X** are reliably measured or if a credible instrumental variable cannot be identified, then the average treatment effect is not identifiable from observational data. Thus, one might first think about an RCT or RD design in order to identify an average treatment effect.

The causal graph for a RCT is shown in Figure 2, where *R* denotes randomization. The assumptions encoded by missing arrows in the graph are the following: i) there is no arrow $R \rightarrow Y$ because randomization must not have a direct effect on *Y* under SUTVA; ii) there is no arrow $\mathbf{X} \rightarrow Z$ because of perfect compliance and no attrition; iii) there is no arrow $R \rightarrow \mathbf{X}$ because **X** should be measured before treatment assignment (i.e., pre-treatment variables). Under those assumptions, we see the graph satisfies the back-door criterion since there is no path between *Z* and *Y* that contains an arrow into *Z* and thus the causal effect is nonparametrically identified (Pearl, 2009). Conversely, if any of those assumptions is not met (that is, we need to draw at least one of the arrows $R \rightarrow Y$, $\mathbf{X} \rightarrow Z$, or $R \rightarrow \mathbf{X}$), then the corresponding back-door paths between *Z* and *Y* make the causal identification infeasible.

Figure 3(1) shows the causal graph for a sharp RD design, where *A* is the continuous assignment variable. Under the absence of noncompliance, the causal graph encodes the assumption that *A* exclusively determines the treatment status *Z*, that is, there is no arrow $\mathbf{X} \rightarrow Z$. However, the graph also implies that the assignment by itself could affect the outcome ($A \rightarrow Y$) or be correlated with other potential confounders ($A \leftrightarrow \mathbf{X}$). Without limiting identification to around of cutoff score, the two back-door paths of i) $Z \leftarrow A \rightarrow Y$, ii) $Z \leftarrow A \leftrightarrow \mathbf{X} \rightarrow Y$ (and the lack of overlap) prevent the causal identification on the effect of *Z* on *Y*. However, identification becomes possible if one investigates the casual effect only in an infinitesimally close neighborhood around the cutoff as represented by the limiting graph at the cutoff score in Figure 3(2). The limiting graph satisfies the back-door criterion and the causal effect is identified. Note that the limiting graph is essentially equivalent to the causal graph of an RCT implying that RD designs are actually RCTs at the cutoff score.

The causal graph of an IV design is depicted in Figure 4. An IV is a variable that affects the outcome *Y* only via treatment *Z* but has otherwise no effect on *Y*. Thus, the graph shows the arrow $IV \rightarrow Z$ but no other arrows between *IV* and other variables (exclusion restriction assumption). The strategy IV designs employ to circumvent the confounding due to **X** is identifying two effects of *IV* on *Z* and *IV* on *Y* rather than trying to directly identify the effect of *Z* on *Y*. Since the effect of *IV* on *Y* (average IV effect; AIVE) is not affected by **X** (graphically, the path $IV \rightarrow Z \leftarrow \mathbf{X} \rightarrow Y$ is naturally blocked due to the collider *Z* on this path), one can calculate the effect of *Z* on *Y* as the ratio between AIVE ($IV \rightarrow Z \rightarrow Y$) and the effect of *IV* on *Z* ($IV \rightarrow Z$). Under the monotonicity or no-defier assumption the treatment effect is identified for the latent subpopulation of compliers (CATE; Angrist, Imbens & Rubin, 1996). To see the mechanics behind the identification of CATEs, we introduce conditional graphs in Figure 5 for latent subgroups of compliers (1) and always takers & never takers (2). By definition, compliers strictly follow the IV's assignment, therefore, there is no arrow $\mathbf{X} \rightarrow Z$, while always takers and never takers are never influenced by the IV, thus, there is no arrow $IV \rightarrow Z$. For the complier graph, the effect $IV \rightarrow Z$ is necessarily equal to 1 (because $Z = IV$) and thus the AIVE is identical to CATE, τ_C, in Figure 6(1). Thus, if the latent subpopulation of compliers would be identifiable, CATE would be directly identified (while the effect for always and never takers cannot be identified without conditioning on **X**). But since we rarely know who the compliers (they are latent) are we only can use the data of compliers, always and never takers together (no defiers) as presented in Figure 5(3). From the no defiers graph, however, the CATE become identifiable under monotonicity assumption, because i) the AIVE ($IV \rightarrow Z \rightarrow Y$) is the product of the complier probability and CATE, that is, $\gamma\tau_C$, ii) the average effect $IV \rightarrow Z$ is given by the complier probability $\gamma = P(S_i = Complier)$, and finally iii) taking the ratio of the two, the effect of *Z* on *Y* is computed by $\frac{\gamma\tau_C}{\gamma} = \tau_C$, which is the CATE. The identification of IV designs can be directly applied to noncompliance issue in RCTs and RD designs (i.e., fuzzy RD designs) as in Figure 7 and 8, respectively.

Finally, Figure 9 and 10 show the causal graphs for matching and PS designs, respectively. In those designs researchers typically are not in control of the selection to treatment. However, if the strong ignorability assumption is met (Rosenbaum & Rubin, 1983), then by conditioning on a matching indicator or the PS the causal effects can be identified. The crucial step in in matching

or PS designs is the computation of the matching indicator or the PS. Since the matching indicator is determined from both the treatment Z and the confounders $\mathbf{X}$ the indicator S necessarily is a collider on the path between Z and $\mathbf{X}$ (Mansournia, Hernán & Greenland, 2013; Shahar & Shahar, 2012; Figure 9(2)). Then conditioning on S creates a collider bias but it exactly offsets the confounding path $\mathbf{X} \rightarrow Z$ (Figure 9(3)) and thus achieves $\mathbf{X} \perp Z \mid S$. Since the resulting graph of the matched data in Figure 9(4) now resembles the graph of an RCT, the causal effect is identified without further conditioning. We argue that the very same mechanics apply to all PS designs in general, that is, regardless of the choice of a specific analytic PS method—matching, stratification, or weighting. Again, since the PS is computed from both Z and $\mathbf{X}$, it is a collider on the path between Z and $\mathbf{X}$ (Figure 10(2)) and creates collider bias once one conditions on it via matching, stratifying or weighting. The collider bias exactly offsets the confounding path (Figure 10(3)) and finally establishes the independence $\mathbf{X} \perp Z \mid PS$ in Figure 10(4).

Conclusions:

This paper presents the causal graphs of experimental and quasi-experimental designs. For quasi-experimental designs we demonstrate that a causal treatment effect can be identified if we can isolate a subpopulation whose graph resembles the graph of an RCT. For RD designs the corresponding subpopulation is given by the population in the very close neighborhood around the cutoff score; For the IV design it is the subpopulation of compliers; For matching designs it is the matched population and for PS stratification or weighting designs it is the stratified or weighted population. The causal graphs also show that the identification of causal effects rests on stronger assumptions as the researchers' control over the study diminishes. More control usually implies simpler the data-generating mechanism and, thus, relative ease of identification.

Appendices

Not included in page count.

Appendix A. References

Angrist, J. D., Imbens, G. W., & Rubin, D. B. (1996). Identification of causal effects using instrumental variables. *Journal of the American Statistical Association, 87,* 328-336.

Elwert, F., & Winship, C. (2014). Endogenous selection bias: the problem of conditioning on a collider variable. *Annual Review of Sociology, 40,* 31-53.

Holland, P. W. (1986). Statistics and causal inference. *Journal of the American Statistical Association, 81,* 945-970.

Mansournia, M. A., Hernán, M. A., & Greenland, S. (2013). Matched designs and causal diagrams. *International Journal of Epidemiology, 42,* 860-869.

Morgan, S. L., & Winship, C. (2014). *Counterfactuals and causal inference: Methods and principles for social research*, 2nd edition. Cambridge: Cambridge University Press.

Pearl, J. (2009). *Causality: Models, Reasoning, and Inference*. Cambridge: Cambridge University Press.

Rosenbaum, P. R., & Rubin, D. B. (1983). The central role of the propensity score in observational studies for causal effects. *Biometrika, 70*(1), 41-55.

Rubin, D. B. (1990). Formal modes of statistical inference for causal effects. *Journal of Statistical Planning and Inference, 25*(3), 279-292.

Shadish, W. R., Cook, T. D., & Campbell, D. T. (2002). *Experimental and Quasi-Experimental Designs for Generalized Causal Inference*. Boston: Houghton-Mifflin.

Shadish. W. R., & Sullivan, K. J. (2012). Theories of causation in psychological science. In Harris Cooper (Ed.), *APA Handbook of Research Methods in Psychology*, Volume 1, 23-52.

Shahar, E., & Shahar, D. J. (2012). Causal diagrams and the logic of matched case-control studies. *Clinical Epidemiology, 4,* 137-144.

Spirtes, P., Glymour, C. N., & Scheines, R. (2000). *Causation, prediction, and search* (Vol. 81). MIT press.

Steiner, P. M., Kim, Y., Hall, C. E., & Su, D. (in press). Graphical Models for Quasi-experimental Designs. *Sociological Methods & Research*, 0049124115582272.

Appendix B. Tables and Figures

Figure 1. Causal graph of an observational study: complete and stylized representation.

(1) Complete graph

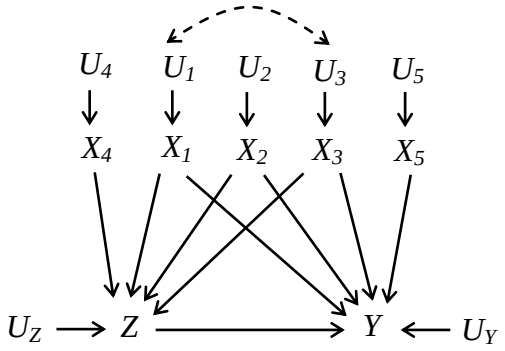

(2) Stylized graph

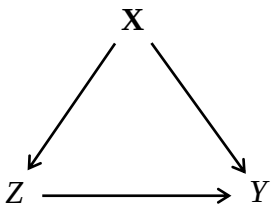

Figure 2. Data generating graph of a randomized controlled trial.

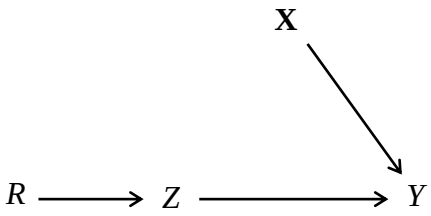

Figure 3. Causal graphs of a regression discontinuity design: (1) data generating graph and (2) limiting graph for $A = a_C \pm \varepsilon$ with $\varepsilon \to 0$.

(1) Data generating graph

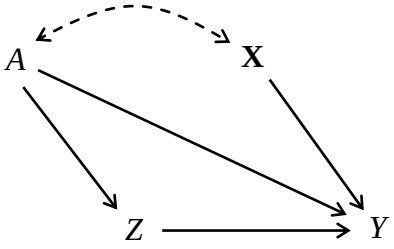

(2) Limiting graph

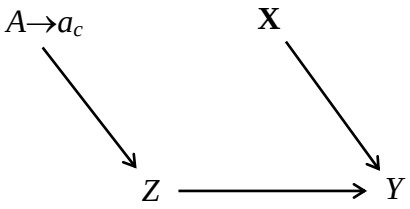

Figure 4. Data generating graph of an instrumental variable design.

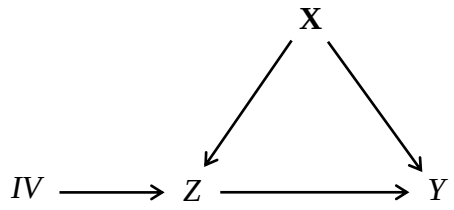

Figure 5. Data generating IV graphs for (1) compliers (C), (2) always takers and never takers (A+N), and (3) compliers, always takers and never takers together (i.e., no defiers).

(1) Compliers (C)

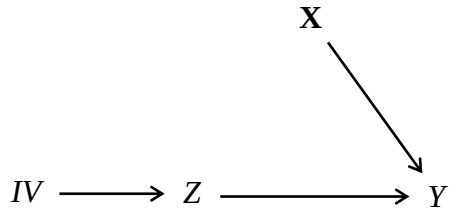

(2) Always takers & never takers (A+N)

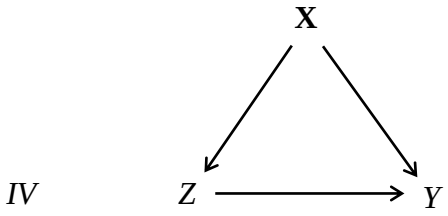

(3) No defiers (C+A+N)

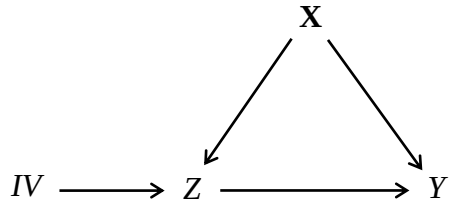

Figure 6. IV graphs for (1) compliers and (2) compliers, always takers and never takers together (i.e., no defiers).

(1) Compliers (C)

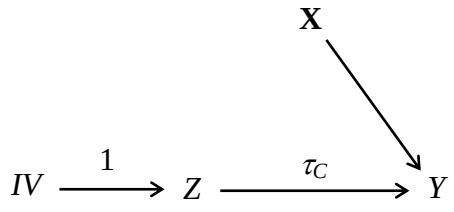

(2) No defiers (C+A+N)

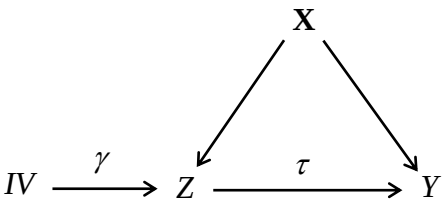

Figure 7. Causal graph of the randomized controlled trial with noncompliance.

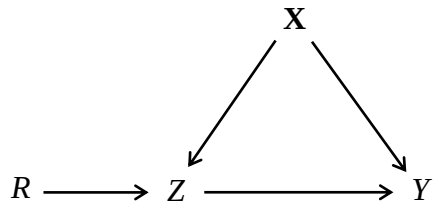

Figure 8. Causal graphs for the fuzzy regression discontinuity design: (1) data generating graph and (2) limiting graph for $A = a_C \pm \varepsilon$ with $\varepsilon \to 0$.

(1) Data generating graph

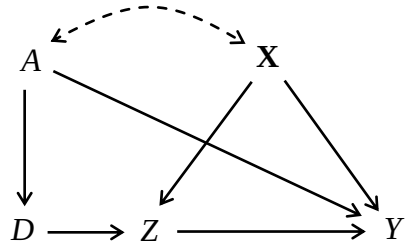

(2) Limiting graph

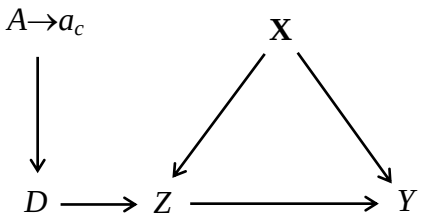

Figure 9. Causal graphs for a matching design (with constant matching ratio): (1) Data generating DAG, (2) computation of match indicator *S*, (3) conditioning on the match indicator *S*, and (4) the independence structure after matching (*S* = 1).

(1) Data generating graph

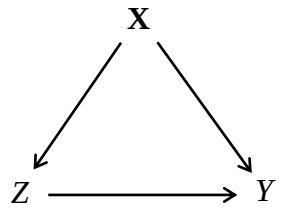

(2) Computation of match indicator

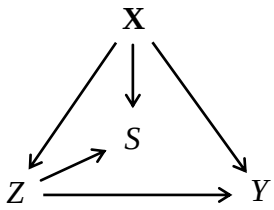

(3) Conditioning on the match indicator

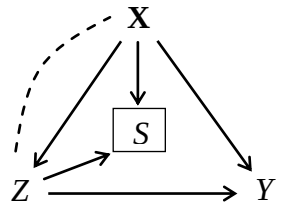

(4) Independence structure after matching (S = 1)

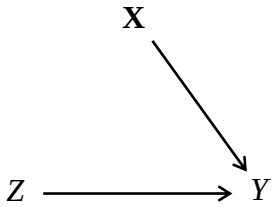

Figure 10. Causal graphs for propensity score designs: (1) Data generating DAG, (2) computation of the propensity score (PS), (3) conditioning on the PS, and (4) the independence structure after PS-adjustment.

(1) Data generating graph

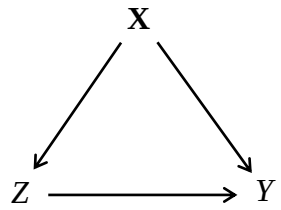

(2) Computation of PS

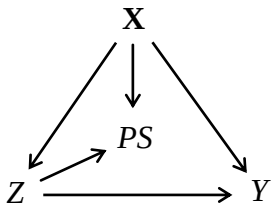

(3) Conditioning on the PS

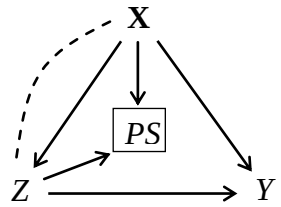

(4) Independence structure after PS adjustment